JOURNAL OF SOLID STATE CHEMISTRY **136,** 175–180 (1998)
ARTICLE NO. SC977671

Crystal Chemistry and Polymorphism of Potassium–Magnesium Monophosphate

G. Wallez,*,[1] C. Colbeau-Justin,* T. Le Mercier,* M. Quarton,* and F. Robert†

*Laboratoire de Cristallochimie du Solide (CNRS-URA 1388) and †Laboratoire de Chimie des Métaux de Transition (CNRS-URA 419), Université Pierre et Marie Curie, 4 Place Jussieu, 75252 Paris Cedex 05, France

Received June 3, 1997; in revised form October 22, 1997; accepted October 23, 1997

The new compound $KMgPO_4$ has been synthesized, and its structure has been determined at room-temperature (α form): space group is $P2_1/c$ (No. 14) with cell parameters $a = 8.549(2)$ Å, $b = 5.078(1)$ Å, $c = 18.996(2)$ Å, $\beta = 91.68(1)°$, and $Z = 8$. Phase transitions occur at 362 and 422°C, β-$KMgPO_4$ and γ-$KMgPO_4$ are orthorhombic, respectively $Pna2_1$ (No. 33) and *Pnma* (No. 62). The β and γ forms are related to the tridymite type, with a skeleton made of MgO_4 and PO_4 tetrahedra, but in α form, half of the magnesium atoms are pentacoordinated.

INTRODUCTION

This work, introducing the new monophosphate $KMgPO_4$ is part of a research program on crystal chemistry and polymorphism of $A^{I}B^{II}PO_4$ compounds. These phases usually consist of a tetrahedra-built BPO_4^- framework (B is a small bivalent cation: Be, Mg, Co, Zn) hosting a large monovalent cation A (K, Tl, Rb, Cs). They commonly crystallize under NH_4LiSO_4 (1) or $KAlGeO_4$ (2) types, themselves belonging to the stuffed tridymite family. Previous studies showed that $AMgPO_4$ (A = Rb, Tl, Cs) compounds adopt the NH_4LiSO_4 cycle topology (3, 4), with tetrahedra following a UUUDDD (U for up, D for down) order along the six-membered rings. They belong to the monoclinic or orthorhombic system but show a clear pseudohexagonal tendency. The ferroelectric character of their polymorphism has also been underscored in several recent works (5, 6).

EXPERIMENTAL PROCEDURES

Synthesis. Elaboration of powder samples of the title compound was achieved by solid-state reaction from pure reagents: $NH_4H_2PO_4$, K_2CO_3 and $(MgCO_3)_4$, $Mg(OH)_2$, $5H_2O$. A stoichiometric mixture, poured in a platinum crucible, was ground several times during progressive annealing in air from 130 to 800°C. Obtained powder is white.

Flux growth. A successful method for elaboration of $KMgPO_4$ single crystals consists in cooling a melt of the same reagents as those used for synthesis, but with stoichiometric proportions allowing in situ formation of both potassium–magnesium monophosphate (60% molar) and potassium diphosphate $K_4P_2O_7$ (40% molar) which will act as flux. The mixture is melted at 1200°C, cooled slowly (3°C h^{-1}) to 1000°C, then faster (10°C h^{-1}) to room temperature. Highly soluble potassium diphosphate is eliminated by washing in distilled water. Crystals are prismatic, transparent, and colorless. This method allows us to carry out crystallization below the melting point of $KMgPO_4$ (1404°C), so losses through evaporation are of lesser importance. It also avoids any risks of pollution by ionic exchange between flux and growing crystals.

Hydrothermal growth. Another way to prepare single crystals is the hydrothermal method. Previously synthesized $KMgPO_4$, used as nutrient, was poured into a 6 cm^3 copper tube, along with a 3 M KOH solution giving a 70% filling ratio. Mineralizer was selected according to two chemical criteria:

- Cationic exchange may occur between solution and compound without any risk of pollution.
- Alkaline solution provides hydroxide anions which increase solubility of nutrient by complexation.

A copper container was placed in a cone-sealed refractory steel vessel, set under 90 MPa nitrogen pressure, and heated to 500°C for 2 days. Pressure around container reached 180 MPa, thus equilibrating the estimated solution pressure on the inner side (7).

Obtained crystals are transparent, colorless, and elongated along b (twofold) axis, with size ranging from 50 to 300 μm along this direction. The use of a 3 M KF solution gave similar results thanks to the high complexation ability

[1]To whom correspondence is to be addressed.

0022-4596/98 $25.00

of fluoride anions. The faces observed by optical goniometry have indexes 012, 210, and $\bar{2}10$ (room temperature monoclinic axes setting).

Structure determination. Weissenberg and precession photographs performed at room temperature on a single crystal showed monoclinic symmetry, with extinctions corresponding to space group $P2_1/c$. Parameter $c = 18.996$ Å is worth twice the usual value observed on most $ABPO_4$; such a superstructure has already been reported for the low-temperature forms of isotypic $CsZnPO_4$ (8) and NH_4LiSO_4 (9) which adopt the same space group.

A quasispherical hydrothermal-grown single crystal with diameter about 200 μm was used for collection of diffracted intensities on a four-circle diffractometer. Experimental parameters are summarized on Table 1.

Because of the small dimensions of crystal and moderate value of linear absorption coefficient ($\mu = 16.88$ cm^{-1}) (10), absorption correction was not necessary. Atoms were located by direct methods (SHELXS-86 (11)), and then positions and anisotropic thermal parameters were refined by the least-squares method (CRYSTALS (12)).

TABLE 1
Data Collection and Refinement Conditions

Crystallographic Data	
Crystal system	Monoclinic
Space group	$P2_1/c$ (No. 14)
Cell parameters (refined from	$a = 8.549(2)$ Å
24 reflections with $18 < \theta < 19°$)	$b = 5.078(1)$ Å
	$c = 18.996(2)$ Å
	$\beta = 91.68(1)°$
Volume/Z	824.3(4)Å^3/Z = 8
Formula weight	158.37 g mol^{-1}
Calculated density	2.55
Linear absorption coefficient	16.88 cm^{-1}
Data Collection	
Diffractometer	Enraf-Nonius CAD-4
Radiation/monochromator	$\lambda_{MoK\alpha} = 0.71069$ Å/graphite
Temperature	293 K
Collection method	ω–2θ
Scan range	$0.8 + 0.345 \tan\theta$
θ limits	$1 < \theta < 35°$
Ranges of collected indexes	0, 13; 0, 8; −30, 30
No. of observed (independent) reflections	4156 (3614)
Decay of standard reflections	< 1%
Refinement	
No. of refined parameters	128
No. of conserved reflections	2992 ($I > 3\sigma(I)$)
Extinction parameter	20.3×10^{-6}
R	0.026
R_w	0.027
Weighting scheme	$w = 1/\sigma(F)$
Goodness of fit	2.8
$\Delta\rho_{min}$, $\Delta\rho_{max}$	−0.46, 0.47e Å^{-3}

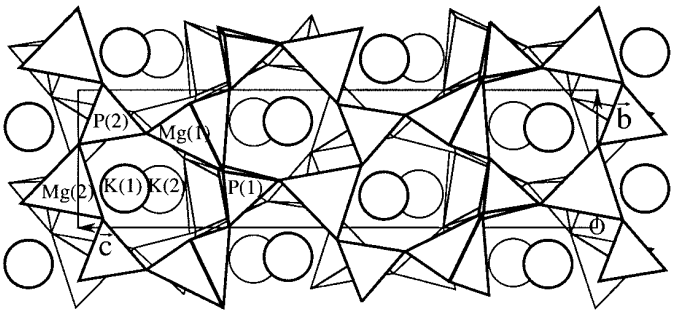

FIG. 1. Projection following a of α-$KMgPO_4$ cell.

STRUCTURE OF α-$KMgPO_4$

Structure description. Unlike all other $A^IB^{II}PO_4$ structures involving small bivalent B cations (B = Be, Mg, Zn) and large monovalent A cations (A = K, Rb, Cs, Tl), the oxygen framework of α-$KMgPO_4$ (Fig. 1) is not exactly made up of corner-bound BO_4 and PO_4 tetrahedra as in the so-called "stuffed-tridymite" structural type: the existence of different oxygen environments for the two magnesium atoms is the most outstanding feature of this structure (Fig. 2). See Table 2 for atomic coordinates and thermal parameters and Tables 3–5 for cationic environments.

Unlike Mg(2), which is located in a tetrahedron showing a slight distortion due to the size of the cation, Mg(1) has a five-oxygen irregular environment resulting from the alteration of the ideal all-tetrahedra framework: the $P(1)O_4$ tetrahedron is tilted by about 45°, allowing Mg(1) and P(1) to share two oxygen atoms (O(1)′ and O(2)). There

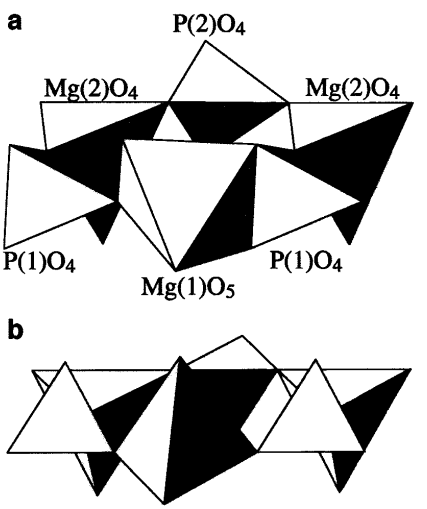

FIG. 2. (a) Oblique view of α-$KMgPO_4$ showing unusual environment of Mg(1) and P(1) atoms and in α-$KMgPO_4$. (b) Oblique view of a classical UUUDDD tetrahedra ring (β and γ forms).

TABLE 2
Fractional Atomic Coordinates and Thermal Parameters

Atom	x	y	z	U_{eq} (Å^2)
K(1)	0.00440(4)	0.72504(9)	0.09327(2)	0.0209(2)
K(2)	0.48209(5)	0.23595(9)	0.34065(2)	0.0232(2)
Mg(1)	0.84365(6)	0.2741(1)	0.23068(3)	0.0092(2)
Mg(2)	0.32309(6)	0.2793(1)	0.03046(3)	0.0111(2)
P(1)	0.20769(4)	0.20576(8)	0.18993(2)	0.0096(1)
P(2)	0.70499(4)	0.24603(8)	0.06278(2)	0.0093(1)
O(1)	0.0509(1)	0.0941(2)	0.21765(6)	0.0123(5)
O(2)	0.3295(1)	0.0378(3)	0.22911(7)	0.0159(6)
O(3)	0.2264(2)	0.4983(3)	0.20557(8)	0.0174(6)
O(4)	0.2078(2)	0.1620(3)	0.11031(6)	0.0198(7)
O(5)	0.7864(2)	0.3169(3)	0.13250(6)	0.0176(6)
O(6)	0.5329(1)	0.3238(3)	0.06619(8)	0.0219(7)
O(7)	0.7806(2)	0.3998(2)	0.00310(6)	0.0163(6)
O(8)	0.7185(2)	0.9496(2)	0.04935(7)	0.0176(6)

is almost no significant effect on phosphorus P(1) environment because of the stiffness of the PO_4 tetrahedron, but the O(1)′–Mg(1)–O(2) angle is very low (68.98°) and the Mg(1)–O(1)′ and Mg(1)–O(2) bonds are longer than usual.

In NH_4LiSO_4-type structures, tunnels perpendicular to six-tetrahedra rings are slightly bent, forming hemispherical coordination polyhedra for the large monovalent cations (13). In α-$KMgPO_4$, the tilt of $P(1)O_4$ tetrahedra induces a slight shift (about 0.7 Å following c axis) of the oxygen layers which modifies the environment of stuffing potassium atoms: $K(1)O_7$ polyhedron is closed but loose (0.83 valence unit shared between K(1) and its neighbors), whereas atom K(2) is strongly bound to an open six-oxygen polyhedron (0.96 vu) (14).

PHASE TRANSITIONS

DSC measurements reveal two high-temperature endothermic reversible phase transitions at 362°C (rev. 353°C) and 422°C (rev. 419°C). Enthalpies are respectively 3.0 and 0.4 J g^{-1}, suggesting a first-order mechanism for the former and a second-order one for the latter.

High-temperature X-ray powder patterns have been recorded for $8 < 2\theta < 80^\circ$ on a Bragg-Brentano diffractometer ($\lambda_{CuK\alpha} = 1.54178$ Å) to explain the transitions in terms of cell modifications. Figure 3 shows two important changes between α and β forms:

- hkl reflections of α form with odd l index vanish in β form, indicating that parameter c is halved.
- $\bar{h}kl$ and hkl reflections are no longer split in high-temperature forms; systematic extinctions allow to give β-$KMgPO_4$ an orthorhombic $Pna2_1$ symmetry and γ-$KMgPO_4$ an orthorhombic $Pnma$ symmetry as for medium- and high-temperature forms of $NH_4LiSO_4^-$ type compound (1, 15) and isotypic monophosphate $CsZnPO_4$ (8). Cell parameters refined from powder patterns and symmetries of varieties β and γ are summarized in Table 6. Note changes in axes setting from one form to the other.

Structural modification. The unusual environment of Mg(1) in α-$KMgPO_4$ distorts the oxygen skeleton which shows therefore a clear deviation from the common pseudohexagonal geometry as can be seen from the $c/2b$ ratio (Table 6). Values pertaining to other A^IMgPO_4 (stuffed-tridymite compounds) are given for comparison.

However, medium- and high-temperature forms clearly adopt a pseudohexagonal geometry, with parameter ratios close to $\sqrt{3}$. This agrees with the halving of the cell volume which imposes identical sites for all magnesium atoms (order of group $Pna2_1$, Z number, and multiplicity of all positions 4). From these results, we can admit that $Mg(1)O_5$ polyhedra only exist in α form, β and γ forms having an all-tetrahedra skeleton. The change of coordination explains the first-order character of α–β transition whereas stuffed-tridymite compounds usually transform via second-order phenomena, as in the case of low-enthalpy β–γ transition.

Ionic conductivity. Stuffed-tridymite type compounds usually show a slight ionic conductivity mainly due to the ability of the A^+ cations to move along the tunnels through the six-membered rings from one site to another. However, the absence of vacant sites does not allow high performance. Tetracoordinated cations are strongly bound to the oxygen framework and therefore play no significant role.

A $KMgPO_4$ sintered pellet has been studied on a Hewlett-Packard 4284A impedancemeter by complex impedance spectrometry. Ionic conductivity was measured from

TABLE 3
Distances (Å) and O–P–O Angles (deg) in PO_4 Tetrahedra

$P(1)O_4$	O(1)	O(2)	O(3)	O(4)	$P(2)O_4$	O(5)	O(6)	O(7)	O(8)
O(1)	1.561(1)	102.32(7)	112.03(7)	107.84(7)	O(5)	1.521(1)	108.58(8)	109.33(8)	110.04(8)
O(2)	2.402(1)	1.523(1)	112.60(8)	112.44(8)	O(6)	2.475(1)	1.527(1)	109.08(8)	109.82(9)
O(3)	2.557(1)	2.534(1)	1.523(1)	109.37(8)	O(7)	2.493(1)	2.494(1)	1.535(1)	109.97(7)
O(4)	2.497(1)	2.537(1)	2.490(1)	1.529(1)	O(8)	2.501(1)	2.502(1)	2.511(1)	1.531(1)

TABLE 4
Distances (Å) and O–Mg–O Angles (deg) in MgO_n Polyhedra

$Mg(1)O_5$	O(1)	O(1)′	O(2)	O(3)	O(5)	$Mg(2)O_4$	O(4)	O(6)	O(7)	O(8)
O(1)	2.015(1)	92.39(3)	160.37(5)	92.15(5)	97.56(6)	O(4)	1.927(1)	104.65(7)	106.10(7)	110.14(6)
O(1)′	2.963(1)	2.089(1)	68.98(5)	113.67(6)	117.45(6)	O(6)	3.039(1)	1.912(1)	115.42(7)	119.88(7)
O(2)	4.107(1)	2.402(1)	2.153(1)	89.97(6)	96.62(6)	O(7)	3.101(1)	3.268(1)	1.953(1)	100.03(6)
O(3)	2.861(1)	3.388(1)	2.908(1)	1.957(1)	127.31(7)	O(8)	3.167(1)	3.330(1)	2.979(1)	1.935(1)
O(5)	2.966(1)	3.433(1)	3.050(1)	3.480(1)	1.927(1)					

Cole–Cole diagrams recorded at stabilized temperature. Figure 4 shows a jump of the conductivity around 362°C, corresponding to an α–β transition. On the $\ln(\sigma, T)$ vs $1000/T$ plot (Fig. 5), linear α and γ domains confirm the ionic nature of the conductivity. As the jump spreads over the narrow stability range of the β form, we can only compute the activation energies from the slopes of the high- and low-temperature straight lines: $E_\alpha = 1.03$ eV and $E_\gamma = 0.82$ eV.

DISCUSSION

Previous works have pointed out that divalent alkali earth or transition cations (M = Mg, Mn, Fe, Co, Ni, Cu, Zn) are likely to adopt various and more or less irregular MO_n ($n = 4, 5, 6$) coordination polyhedra in monophosphates, number n being subject to changes with phase transitions (16, 17). As these structures are not based on close-packed oxygen sublattices, cations are not systematically located in regular tetrahedra or octahedra. Furthermore, $M^{II}O_4$ tetrahedra are less stable than XO_4 ones (X is a posttransition cation) because of the higher ionic radius of M^{II} cations and the less covalent nature of the M–O bond.

So, pentacoordinated magnesium atoms are conceivable in the noncompact framework of α-$KMgPO_4$ (25.76 $Å^3$ per oxygen atom), although such an environment is considered as rare by A. G. Nord *et al.* (16). To our knowledge, it is the only one among tridymite-related compounds to this date.

TABLE 5
Distances (Å) around K Atoms

K(1)–O(7)	2.707(1)	K(2)–O(2)	2.612(1)
O(8)	2.802(1)	O(2)	2.654(1)
O(4)	2.832(1)	O(6)	2.746(1)
O(5)	2.899(1)	O(3)	2.927(1)
O(7)	3.022(1)	O(8)	2.948(1)
O(1)	3.033(1)	O(5)	3.182(1)
O(3)	3.040(1)		
		O(6)	3.474(1)
O(4)	3.357(1)		

For this formula type, the most symmetrical structure is the pseudohexagonal *Pnma* form of NH_4LiSO_4 (1). As the transitions proceed from tetrahedra reorientations at heating, we can suppose that tetrahedron $P(1)O_4$ rotates away from its very tilted direction to become perpendicular to the oxygen layers, removing the fifth oxygen from atom Mg(1), as seen in Figs. 2a and 2b. Cell is halved, as all magnesium atoms become identical. So, the change of coordination results of a more general process of symmetry increasing.

This structural feature is unique among $AMgPO_4$ (A = K, Rb, Cs) monophosphates and probably stems from the smaller ionic radius of potassium cation ($r_{i(K^+)} = 1.51$ Å; $r_{i(Rb^+)} = 1.61$ Å; $r_{i(Cs^+)} = 1.74$ Å in 8-coordination) (18) which increases transition temperatures: ambient forms of $RbMgPO_4$ (3) and $CsMgPO_4$ (3) are respectively analogous with β-$KMgPO_4$ and γ-$KMgPO_4$ in which magnesium can only be tetracoordinated. Actually, a tridymite framework tends to adopt a higher symmetry if the stuffing cation is bulky, that is, if it fully fills the large cavities. Low-temperature diffraction would be necessary to study α-$RbMgPO_4$

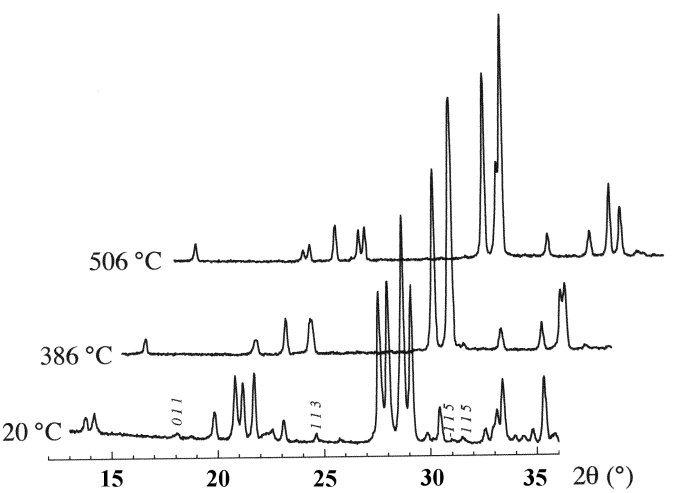

FIG. 3. X-ray powder patterns of α (20°C), β (386°C), and γ-$KMgPO_4$ (506°C) showing disappearance of *hkl*, *l* odd reflections.

TABLE 6
Cell Parameters and Ratios of $AMgPO_4$ Compounds (A = Tl, Rb, Cs) at Room Temperature and the Three Forms of $KMgPO_4$

Compound	Space group	a, b, c (Å)	β (deg)	Ratio
α-$KMgPO_4$		8.549(2)		
	$P2_1/c$	5.078(1)	91.68(1)	$c/2b = 1.08\sqrt{3}$
		18.996(2)		
β-$KMgPO_4$		8.586(1)		
(386°C)	$Pna2_1$	9.254(1)		$b/c = 1.01\sqrt{3}$
		5.2955(7)		
γ-$KMgPO_4$		8.645(1)		
(506°C)	$Pnma$	5.2785(7)		$c/b = 1.02\sqrt{3}$
		9.335(1)		
$RbMgPO_4$ (3)		8.840(1)		
	$Pna2_1$	9.291(1)		$b/c = 1.01\sqrt{3}$
		5.3359(6)		
$TlMgPO_4$ (4)		8.3826(4)		
	$P2_1$	5.3361(2)	91.910(4)	$c/b = 1.03\sqrt{3}$
		9.5376(4)		
$CsMgPO_4$ (3)		8.935(2)		
	$Pnma$	5.526(1)		$c/b = 1.01\sqrt{3}$
		9.646(2)		

and α-$CsMgPO_4$, but one can doubt that Rb^+ and Cs^+ may fit in a site reduced by the collapsing of the oxygen framework resulting of the existence of MgO_5 polyhedra. The case of $TlMgPO_4$ is somewhat different because of the higher electronegativity and the stereochemical activity of the $6s^2$ lone pair of thallium, so it cannot be put forward for comparison.

The shape of the ionic conductivity curve of $KMgPO_4$ finds its explanation in the α–β transition mechanism. The shift of the (100) planes reduces the cross-section of the tunnels and increases the activation energy of the K^+ hopping. As Mg(1) becomes tetracoordinated in β and γ forms, tunnels become straighter and broader, allowing ionic conductivity to increase and activation energy to reduce. Tunnel cross-sections of the three forms are given on Fig. 6

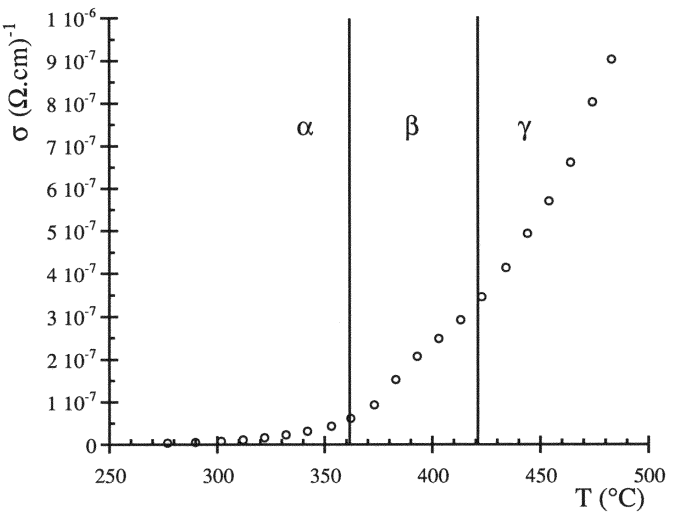

FIG. 4. Thermal variation of the ionic conductivity.

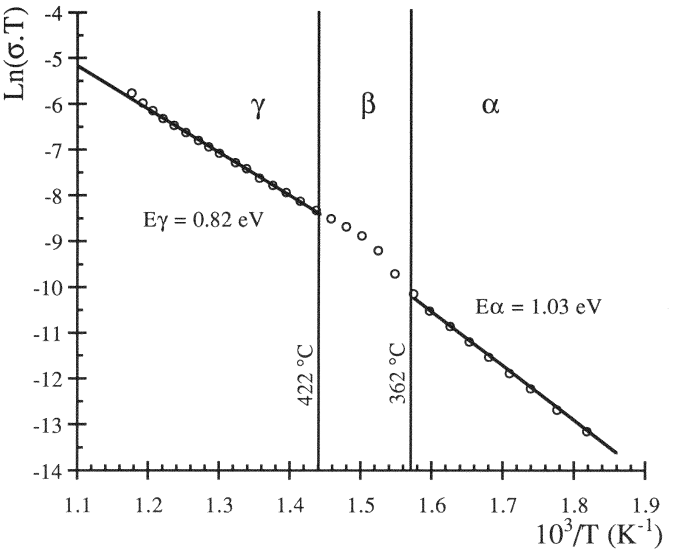

FIG. 5. Ln(σ, T) vs 1000/T plot.

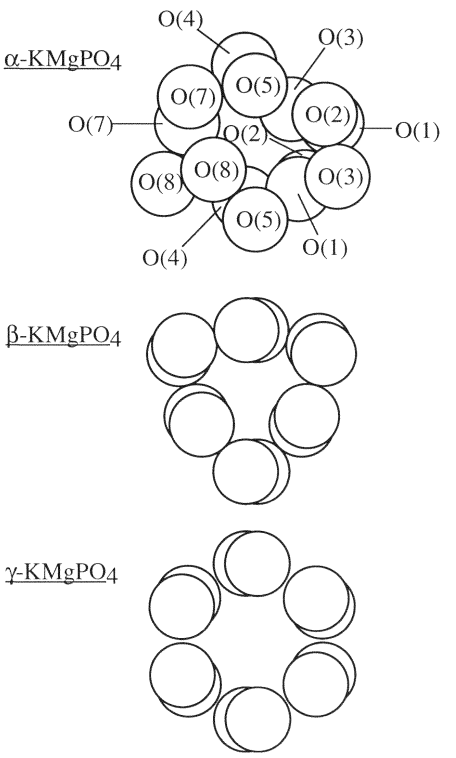

FIG. 6. Tunnel cross-sections of α, β, and γ forms.

(atomic coordinates in β- and γ-$KMgPO_4$ have been roughly computed from cell parameters, the usual sizes of PO_4 and MgO_4 tetrahedra, and by comparison with isotypic compounds).

CONCLUSION

The presence of potassium in the cavities of the $M^{II}PO_4^-$ framework leads to the low-symmetry monoclinic form at room temperature which allows magnesium to adopt a five-oxygen environment more convenient for its large size. This configuration vanishes at high temperature, showing that stabilization of the whole framework by symmetry increasing prevails on the preference of magnesium for a larger coordination polyhedron.

The distortion also affects the environment of potassium cations and their ability to move along the tunnels, generating a notable increase of the ionic conductivity at the α–β transition.

REFERENCES

1. W. A. Dollase, *Acta Crystallogr. B* **25,** 2298 (1969).
2. G. Lampert and R. Böhme, *Z. Kristallogr.* **176,** 29 (1986).
3. E. L. Rakotomahanina Ralaisoa, Thèse, Université de Grenoble, France, 1972.
4. G. Wallez, A. Elfakir, A.-M. Xuriguera, and M. Quarton, *Powder Diffraction* **8,** 145 (1993).
5. D. Blum, J.-C. Peuzin, and J.-Y. Henry, *Ferroelectrics* **61,** 265 (1984).
6. B. Elouadi, L. Elammari, and J. Ravez, *Ferroelectrics* **56,** 17 (1984).
7. G. C. Kennedy, *Am. J. Sci.* **248,** 540 (1950).
8. D. Blum, A. Durif, and M.-T. Averbuch-Pouchot, *Ferroelectrics* **69,** 283 (1986).
9. A. I. Kruglik, M. A. Simonov, and K. S. Aleksandrov, *Sov. Phys. Cryst.* **23,** 274 (1978).
10. "International Tables for X-Ray Crystallography," Vol. IV. Kynoch Press, Birmingham, England, 1974.
11. G. M. Sheldrick, "SHELXS-86: A Program for Crystal Structure Determination." Universität Göttingen, Germany, 1986.
12. D. J. Watkin, J. R. Carruthers, and P. W. Betteridge, "Crystal Users Guide." Chemical Crystallography Laboratory, Oxford University, England, 1985.
13. S. Jaulmes, G. Wallez, A. Elfakir, and M. Quarton, *Eur. J. Solid State Chem.* **30,** 1007 (1993).
14. I. D. Brown and K. K. Wu, *Acta Crystallogr. B* **32,** 1957 (1976).
15. K. Itoh, H. Ishimura, and E. Nakamura, *Acta Crystallogr. B* **37,** 664 (1981).
16. A. G. Nord and P. Kierkegaard, *Chem. Scr.* **15,** 27 (1980).
17. S. Jaulmes, A. Elfakir, M. Quarton, F. Brunet, and C. Chopin, *J. Solid State Chem.* [In press]
18. R. D. Shannon, *Acta Crystallogr. A* **32,** 751 (1976).